International Journal of Innovative Technology and Exploring Engineering (IJITEE)
ISSN: 2278-3075 (Online), Volume-9 Issue-3, January 2020

Multi-Objective Flower Pollination Algorithm Based Controller for UPQC Including Hybrid Power Source

K. Hussain, Puli Sridhar

Abstract*: This paper presents a new control method for Unified Power Quality Conditioner (UPQC) for effective management of the power-sharing and improvement of the quality of power. The voltage disturbances produced in the source side due to non-linear load conditions can be protected using the UPQC model. Flexible Alternating Current Transmission System (FACTS) devices were fed through a hybrid power generator that had the primary source, a Proton Exchange Membrane Fuel Cell (PEMFC) and a secondary source, a supercapacitor. In this paper, a multi-objective function (power factor, voltage sag, and the total harmonic distortion (THD)) with different control strategies have been considered. An optimization algorithm named Flower Pollination Algorithm (FPA) has used for optimizing Proportional Integral (PI) coefficients. A suitable fitness function has been developed for the FPA method and the simulation performed. The performance of the FPA method has been compared with three different algorithms, namely, particle swarm optimization algorithm (PSOA), Differential Evolution Algorithm (DEA), and Ant Colony Optimization Algorithm (ACOA). The result obtained shows the proposed FPA providing the best result compared to other methods.

***Keywords: multi objective function, flower pollination algorithm, UPQC, total harmonic distortion, power sharing*.**

I. INTRODUCTION

In recent years, the quality and the stability of power have been on the increase due to the semiconductor devices that have seen introduction in various electrical power systems. These devices include uninterruptible power supply, adjustable speed drives, lighting drives, and computer power supplies. The non-linear current and voltage was introduced by the load lead for harmonic distortion. It had an effect on all the electrical and electronic equipments due to the poor quality of power. Occurrence of voltage unbalance was seen among the three phases due to load detaching and sudden load activation.

Revised Manuscript Received on January 30, 2020.
***** Correspondence Author
K. Hussain*, Department of Electrical Engineering, Sharad Institute of Technology College of Engineering, Yadrav (Ichalkaranji), Kolhapur (Dist.), Maharashtra, India. Email: hussain16679@gmail.com
Puli Sridhar, Department of Electrical and Electronics Engineering, TRR College of Engineering, Patancheru, Telangana, India. Email: sridhar122879@gmail.com

Maintenance of power quality and steady-state voltage is an important issue in any electrical power system [1].

Various researches have been performed and the results have shown the UPQC as an inexpensive and traditional device used for the protection of the load from the power quality distortion at the common coupling point [2]. The control loops of the UPQC consist of various controllers while the synchronous reference frame (SRF) contains the voltage control loop of the UPQC. The design of UPQC is very simple but cancels the steady-state error. However, the effectiveness of the controller is poor when the harmonic components are included in the signal [3].

The αβ stationary frame that consists of a voltage control loop is implemented using a proportional-resonant controller. On the other hand, the dq rotating frame contains another resonant controller [4]. The conventional Proportional Integral (PI) controller is used for controlling the current, implemented in the abc stationary reference frame [5]. The quarter of the Series Converter (SC) switching frequency is set at the 0 dB of the crossover frequency of the control system for discarding the harmonic components. The rejection of the harmonic is not effective when the noise of the converter switching is not properly attenuated [6,7]. The SRF that contains the conventional PI controller is used when the UPQC operates at a dual compensating strategy [8]. The THD of the grid current is considerably higher when the UPQC is supplied distorted voltage and the grid current is less when the UPQC is supply at pure sinusoidal voltage. The single-phase UPQC is modeled as a single multivariable system and disturbances are refused with the help of the feed-forward signal. The Kalman filter is used for obtaining the signal in the harmonics up to the 29th order [9].

Resonant controllers are widely used to suppress harmonic components and provide efficient performance in electrical power applications [10,11]. This system can be represented by a second-order system with a specifically tuned frequency for ensuring steady-state error. Multi resonant controllers are used when the disturbance has multiple frequencies of the fundamental frequency. Typically, the multi resonant controllers are connected in parallel with the conventional PI or P controllers [12]. A PI-multi resonant controller was used for getting an adequate and robust performance of a system. A low pass filter was connected in series with the controller to avoid switching frequency and when the operating frequencies of the controller are very close. This provides a phase delay in the operation of the controller [13].

Literature [11], shows employment of multi resonant controller and estimation of the state matrix and the state-feedback gain. Moreover, the controller does not have an integrator. It is therefore difficult to ensure the zero steady-state error in the continuous reference frame. Although it provides robust

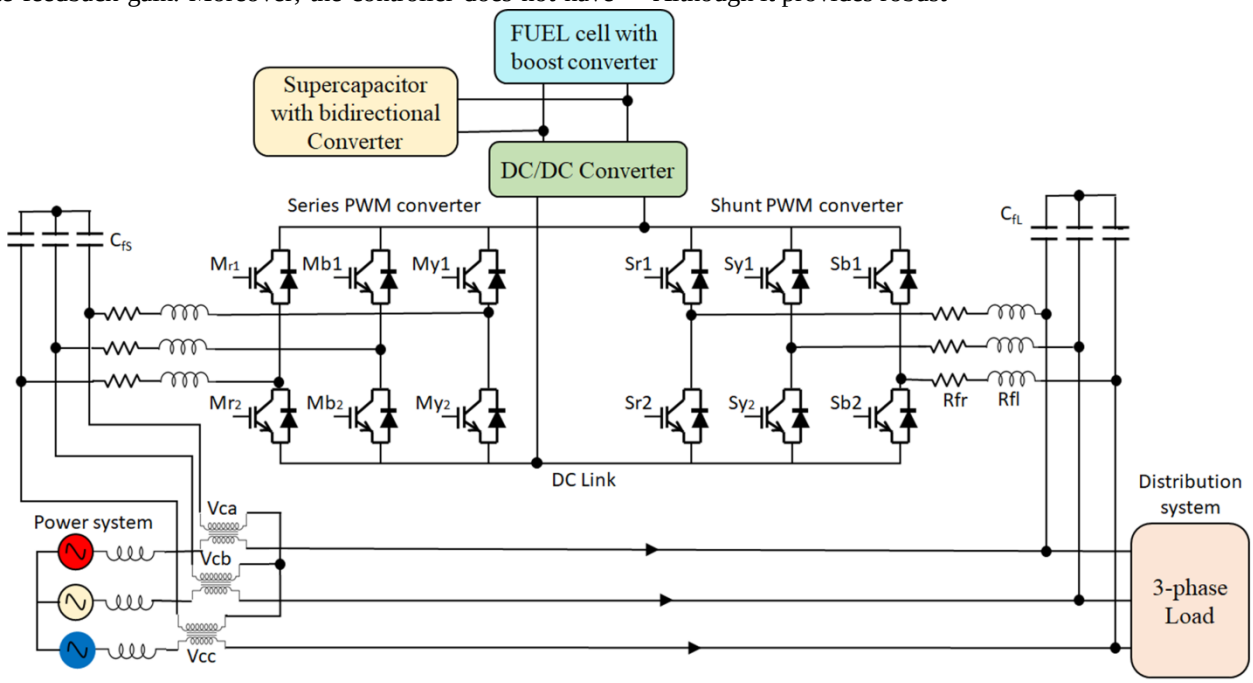

Fig. 1. Structure of UPQC including PEMFC/SC

output, the gain of the controller is not adjusted to compensate for the disturbance. A constrained controller was used for minimizing external disturbance and model uncertainty [14]. The control parameters were updated on the basis of the learning technique used. This helped ensuring the stability of the system under external disturbance and/or uncertainty. A novel robust controller proposd by Zhang et al. provides guaranteed stability under the unstable condition with some delay [15]. Thus, the performance of the system is enhanced with the introduction of the controller using optimization and mirror-mapping methods. Different controllers such as active disturbance rejection controller (ADRC) [16] and modified ADRC were used for compensating for the disturbances seen in the grid-connected system [17]. Adaptive control with simple structure has been sugessted by Kanjiya et al. to control dynamic voltage restorer including high capability [18].

The optimization technique is widely used in the power system for the global optimum problem. The flower pollination algorithm (FPA) has been recognized as an efficient method for solving complicated power system problems. FPA also provides a better solution in the power quality analysis compared to other classical methods [19]. The main contribution of this paper is the evaluation of the performance of the proposed FPA method for improving the quality of power by solving a multi-objective function. The voltage sag, power factor, and the THD have been included in the objective function [20]. Increase in the stability of the controller, it should respond properly under critical situations (fault). The multi-objective DEA algorithm [21] also used in power system analysis. In this paper, a multi-objective function has been developed to enable achievement of accurate load current, reduced voltage, and THD [22]. During this work, the optimization method FPA was introduced and a study of the performance was made. A comparison of these optimization algorithms was made for the evaluation of the effectiveness of the proposed FPA controller. The environmental friendly electrochemical energy sources such as a high power source called supercapacitor (SC) and the high energy source called fuel cell were used [23]. The hybrid source (fuel cell and supercapacitor) is an economically feasible and emerging option for the UPQC system. The remaining of this paper is organized as follows: Section 2 describes the structure and the configuration of UPQC. The mathematical model of the hybrid power source is presented in Section 3. The optimization algorithm with an objective function is described in Section 4. In Section 5, simulation and performance comparison are presented. Conclusions are presented in Section 6.

II. STRUCTURE AND CONFIGURATION OF UPQC

The proposed configuration of UPQC including PEMFC and SC shown in Fig. 1.

It consists of back to back connected two 3-phase Voltage Source Inverters (VSIs) for sharing supply from the hybrid source and a series and shunt active filter. The UPQC was used for compensating voltage fluctuations, voltage fluctuations of power supply, and avert the harmonics of the load current.

It is a traditional power device used for obviating disturbances that have a direct effect on the performance of the critical loads [24,25]. In addition, it has the capability to compensate series and shunt harmonics, power flow control, reactive power, and voltage disturbances including flicker, swell, sag, etc. [2]. The shunt and series active devices were used for the removal of the harmonic current produced by the nonlinear load and adjusting the load voltage respectively.

Fig. 1 shows the C_{FS} and L_{FS} present in the series device acting as a low pass filter (LPF) and filters the output of a series Pulse Width Modulation (PWM) converter. Conversely, the C_{FL} and L_{FL} present in the shunt device act as a LPF and filter the output voltage of the shunt PWM converter. The supercapacitor, interconnected between the fuel cell and the UPQC was shared by the shunt and the series devices. The structure of UPQC including PEMFC/SC is shown in Fig. 1.

The integration of non-linear loads affected the electrical distribution due to the current harmonics and the reactive power of the load. The transformation technique was used for controlling the active-reactive current of the 3-phase shunt converter [26]. The abc-dq0 transformation was used for converting the 3-phase load current into 2-phase active and reactive current components. The load current of the d-axis (I_{Ld}) consists of oscillating and average components. A high pass filter was used for filtering the average part and the load current of the q-axis [27].

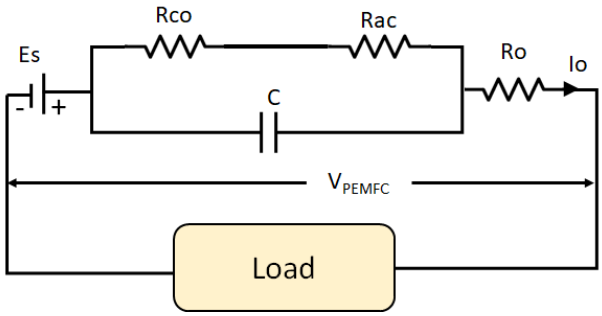

Fig. 2. Equivalent circuit model of PEMFC.

The main aim of the proposed strategy was the estimation of an exact switching for the inverter based on the reference current calculation and voltage sag detection. The supply voltage ($V_s(t)$) that produces the load current ($I_L(t)$), contains the harmonic components of h_1, and the next set of components $h_2$does not have the current components. The non-linearity of the load, resulted in having a set of current components, h_3. Now, $V_s(t)$ and $I_L(t)$ can be expressed as:

$$V_s(t) = \sqrt{2}\left[\sum_{h=1}^{h_1} V_{sh}\sin(h\omega t+\alpha_h)+\sum_{h=1}^{h_2} V_{sh}\sin(h\omega t+\alpha_h)\right] \quad (1)$$

$$I_L(t) = \sqrt{2}\left[\sum_{h=1}^{h_1} I_{sh}\sin(h\omega t+\alpha_h-\psi_h)+ h=1h3Ishsinhωt+αh−ψh\right. \quad (2)$$

Where V_{sh} and I_{sh} represent the rms voltage and current of the h^{th} component. α_h, ψ_h represents the supply voltage random angle and phase angle of the h^{th} harmonic current respectively. In this work, PEMFC and SC were used with UPQC for mitigating electrical perturbation of all kinds associated with the quality of power. Moreover, the shunt active power filter excerpt power from the hybrid source (PEMFC/SC) and provided the required load current. The abc-dq0 transformation was used for converting the 3-phase load current into two-phase active and reactive current components. The I_{Ld} consists of both the oscillating and average components. The high pass filter was used for averaging parts and the oscillating active current was added to the UPQC loss current (i_0). This is expressed based on [28] as:

$$\begin{bmatrix} i_0 \\ i_d \\ i_q \end{bmatrix} = \begin{bmatrix} \frac{1}{\sqrt{2}} & \frac{1}{\sqrt{2}} & \frac{1}{\sqrt{2}} \\ sin\,\omega t & sin\left(\omega t-\frac{2\pi}{3}\right) & sin\left(\omega t+\frac{2\pi}{3}\right) \\ cos\,\omega t & cos\left(\omega t-\frac{2\pi}{3}\right) & cos\left(\omega t+\frac{2\pi}{3}\right) \end{bmatrix} \begin{bmatrix} i_a \\ i_b \\ i_c \end{bmatrix} \quad (3)$$

The oscillating q-axis current was used to generate the compensating current. The dq0-abc transformation was used for converting the q-axis compensating components into 3-phase compensating current. This can be expressed based on [29] as:

$$\begin{bmatrix} i_a \\ i_b \\ i_c \end{bmatrix} = \begin{bmatrix} cos\,\omega t & -sin\,(\omega t) & 1 \\ cos\left(\omega t-\frac{2\pi}{3}\right) & -sin\left(\omega t-\frac{2\pi}{3}\right) & 1 \\ cos\left(\omega t+\frac{2\pi}{3}\right) & -sin\left(\omega t+\frac{2\pi}{3}\right) & 1 \end{bmatrix} \begin{bmatrix} i_d \\ i_q \\ i_0 \end{bmatrix} \quad (4)$$

The switching pulse required for the shunt converter produced by the PI controller was compared with the actual compensating current to the reference compensating current. The series device was used for adjusting the voltage exerted on the load voltage by filtering the utility voltage for producing good sinusoidal voltage and eliminating utility harmonic voltage. The three-phase reference of the series converter load voltage is given by:

$$V_{La}^{*} = V_{dref}\sin(\omega t+\gamma) \quad (5)$$

$$V_{Lb}^{*} = V_{dref}\sin(\omega t+\gamma-120) \quad (6)$$

$$V_{La}^{*} = V_{dref}\sin(\omega t+\gamma-240) \quad (7)$$

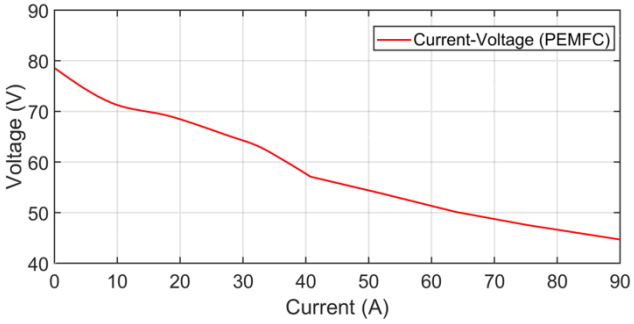

Fig. 3. Relationship between the current and the voltage of the fuel cell

III. MATHEMATICAL MODEL OF HYBRID POWER SOURCE

A. Modeling of PEMFC

PEMFC, also known as polymer electrolyte membrane fuel cell, is a type of electrochemical energy conversion device. It converts chemical energy to electrical energy and thermal energy to a chemical reaction. The simulation model developed revealed the presence of the relationship between the output voltage and partial pressure of hydrogen, current, and oxygen [30]. The output voltage of the stack (V_{st}) can be expressed based on [31] as:

$$V_{St} = E_{RV} - V_{OVL} - V_{CVL} - V_{AVL} \quad (8)$$

$$V_{St} = E_{RV} - N\left[R_{ohm}(i+i_n)+\frac{RT}{\alpha F}ln\left(\frac{i+i_n}{i_o}\right)+ RTβFlniLiL−i+in\right. \quad (9)$$

Where E_{RV} represents the reversible voltage, V_{OVL} is the Ohmic voltage loss,

V_{CVL} is the concentration voltage loss, V_{AVL} is the activation voltage loss. The reversible voltage at varying pressure and temperature can be expressed as:

$$E_{RV} = N\left[E^o + \frac{RT}{2F} ln\left(\frac{P_{H2}(P_{o2})^{1/2}}{P_{H2}o}\right) + \frac{\Delta S_{298.15K}}{\beta F}(T - 298.15)\right] \quad (10)$$

The equivalent circuit of PEMFC was developed on the basis of equation 1 and 2. This is shown in Fig. 2. C represents the equivalent capacitor produced by the double-layer charging effect; R_{co}, R_{ac}, and R_o represent the activation resistance, concentration resistance, and Ohmic resistance respectively.

Oxygen and hydrogen were fed at suitable rates to the PEMFC based on the current and voltage drawn from the load. The reaction of the anode was higher than that of the cathode. This enabled supply of lower stoichiometric flow of air at the anode side. The PEMFC voltage depends on the stoichiometric flow rate of the air, and hence a fan was incorporated to maintain the airflow through the system [32]. An optimal speed controller with three fans and a thermal controller were used for controlling the variable amount of air and maintaining the internal temperature [33]. Moreover, the stack output power (P_{st}) can be expressed as:

$$P_{st} = V_{st}.I \quad (11)$$

Where V_{st} and I represent the output voltage and current of the stack respectively. The relationship between the current and the voltage of the fuel cell is shown in Fig. 3.

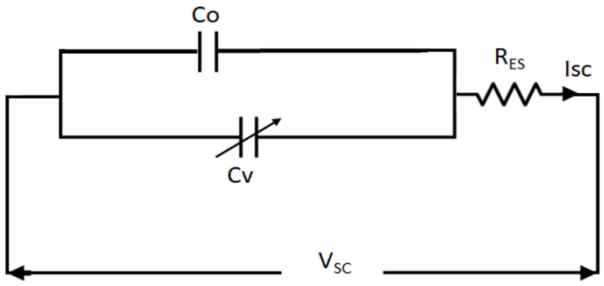

Fig. 4. Equivalent circuit of a supercapacitor.

B. Modeling of Super Capacitor

The fuel cells were connected with the electrochemical energy storage device, the supercapacitor. The SC is a reversible storage device that has high energy density compared to conventional capacitors [34]. So, the feasibility of auxiliary devices based on supercapacitor was high and provide the best solution. Therefore, linking with the PEMFC was found suitable for getting a fast response. Conversely, the fuel cell is called the principal source, whereas the SC bank is the secondary source.

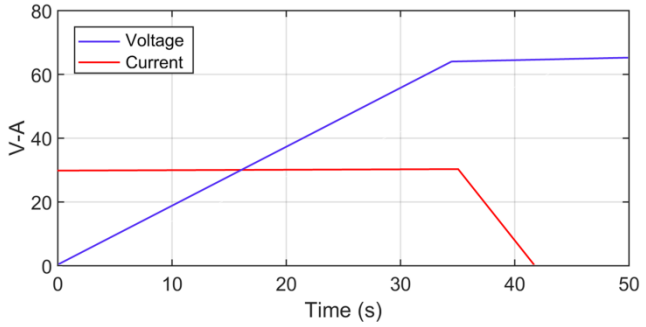

Fig. 5. Relationship between the voltage and current of a supercapacitor.

The basic RC model of the supercapacitor is shown in Fig. 4. This model consists of a variable capacitor (C_V) that is connected in series with the resistance R_{ES}. The relation between the voltage and the current of the supercapacitor is shown in Fig. 5.

C. Multi-Objective Function

Optimization techniques were used in the designing of the controllers for perfect reaction under various fault conditions. In this study, three different objective functions were considered based on the requirement of the problem.

Objective 1: Voltage Sag

In order to minimize the difference between real bus, voltage and the reference bus voltage was led for speedy mitigation of the voltage sag. The deviation present in the voltage can be expressed as:

$$V_d = max|V_R - V_M| \quad (12)$$

There is the requirement for the bus voltage to follow the IEEE-519 standard and the value between 0.95 and 1.05. So the membership function (μ_{GM}) can be developed and it can be expressed as:

$$\mu_{GM} = \begin{cases} \frac{K_{max}-K}{K_{max}-K_{min}}, & for\ K_{min} \le K \le K_{max} \\ 1 & for\ K \le K_{min} \\ 0 & for\ K \ge K_{max} \end{cases} \quad (13)$$

Objective 2: Power factor

A reduction in the phase difference between the current and voltage leads to improvement in the power factor. Most of the real-time loads require some amount of reactive power as the major loads are inductive in nature. The capacitor bank connected in parallel to the load provided reactive power. There was an increase in the power factor and the total apparent input power. Therefore, the apparent power was taken as a fitness function, minimization of apparent input power leading to minimization of power factor [35,36].

The apparent power for single-phase can be expressed as:

$$P_1 = V_1 I_1 \sqrt{\sum_{n=1}^{N} V_{dv1}^2 \times \sum_{n=1}^{N} I_{dc1}^2} \quad (14)$$

Where V_{dv1} and I_{dc1}represent the rms voltage and current of the n^{th} components of phase 1. The objective function of the shunt active filter can be expressed as:

$$O_{sh1} = \sqrt{\sum_{n=1}^{N} V_{dv1}^2 \times \sum_{n=1}^{N} R_{dc1}^2 . V_{dv1}^2} \quad (15)$$

Where $I_{dc1}=R_{dc1}.V_{dc1}$. The optimization method should satisfy the following equality and inequality constraints.

Equality constraints:

The source supplies the mean value of the instantaneous real power based on the demand for the load when compensation is achieved by the shunt active power. The compensating circuit supplies the remaining power. The equality constraint for the mean value of instantaneous real power for a single-phase can be expressed as:

$$\sum_{n=1}^{N} V_{dv1} \times I_{dc1} = \sum_{n=1}^{N} V_{dv1}^2 \times R_{dc1} \quad (16)$$

The equality constraint for the shunt active filter (E_{sh1}) can be expressed as:

$$E_{sh1} = \frac{P}{3} - \sum_{n=1}^{n} V_{dv1}^2 \times \mathrm{R_{dc1}} = 0 \quad (17)$$

Inequality constraints

The THD present in the current should be limited. So the inequality constraint for the THD can be expressed as:

$$E_{sh2} = \sum_{n=2}^{n} R_{dc1}^2 . V_{dv1}^2 - I_{THD}^2 . R_{dc1}^2 V_{dv1}^2 \leq 0 \quad (18)$$

Objective 3: THD

Total harmonic distortion minimization is very important when voltage sag occurs. The THD provides undesirable effects on the connected loads and the membership function can be expressed by the following equation as:

$$\mu_{THD} = \begin{cases} \frac{M_{max} - M}{M_{max} - M_{min}}, & for\ M_{min} \leq M \leq M_{max} \\ 1 & for\ M \leq M_{min} \\ 0 & for\ M \geq M_{max} \end{cases} \quad (19)$$

Multi-objective functions such as GM, sh, and THD uses the FPA optimization algorithm. Getting optimum value requires the maintenance of a minimum value of the objective function.

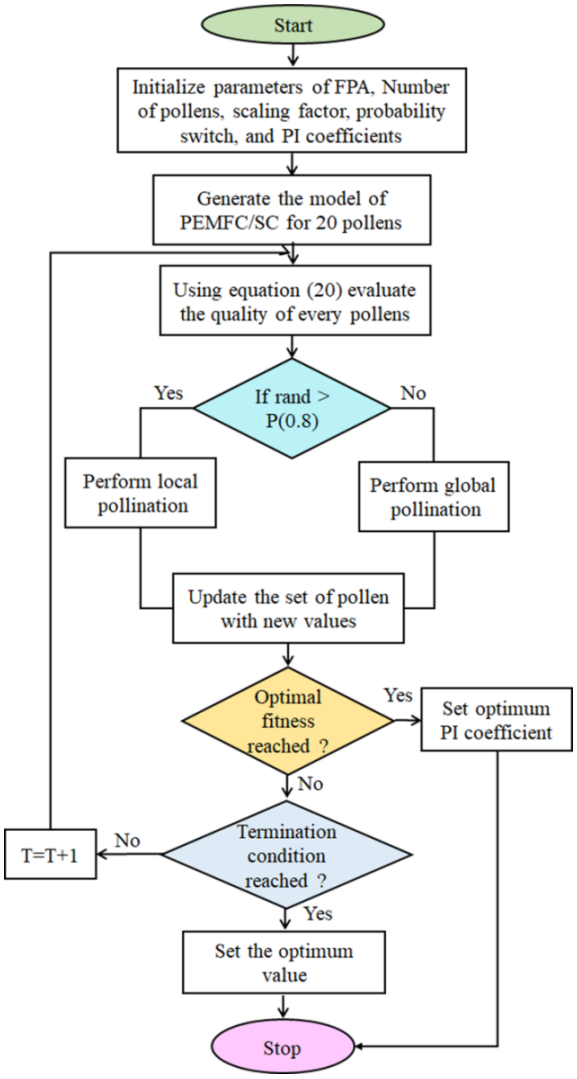

Fig. 6. Flow diagram of FPA algorithm

IV. FPA ALGORITHM

FPA optimization algorithm was developed in the year 2012 by Yang et al. The fundamental process of the FPA algorithm involves the handing over of the pollens from one species to another. Typically, cross-pollination (abiotic) and self-pollinations (biotic) occur in this process. Pollination that occurs from the pollen of different plants is called cross-pollination and pollination that happens between the pollen in the same species is called self-pollination [19]. Cross-pollination is more widely used than self-pollination. The multi-objectives can be formulated as M=[μ_{GM}, P, O_{sh}, μ_{THD}]. FPA adopts different rules to achieve the best solution for the optimization problem is listed below:

Rule 1: The global pollination (exploration) process is characterized by cross-pollination. Levy flight is used by the cross-pollination process for transfer of the pollen from one flower to another. It can be mathematically expressed based on [20] as:

$$M_i^{x+1} = M_i^x + \beta L(G_{best} - M_i^x) \quad (20)$$

Where G_{best} represents the global best solution achieved by the pollens, β and L represent the scaling factor and Levy factor respectively.

Rule 2: The local pollination also called self-pollination is characterized by [21]:

$$M_i^{x+1} = M_i^x + \delta\left(M_j^x - M_k^x\right) \quad (21)$$

$M_j^x and\ M_k^x$ represents different pollens of the same species, δ is the uniform distribution for the local search, $\delta \epsilon [0,1]$.

Rule 3: The switching between the global and local pollination control factor is called the probability switch $P \epsilon [0,1]$. 0.8 has been chosen as the optimal value of the P based on the findings seen in the relevant literature. The flow diagram of FPA algorithm is shown in Fig. 6.

A. Proposed Approach

In this study, the FPA optimization algorithm has been used for minimizing the objective function. During electrical fault conditions such as voltage and current harmonic distortion, swell voltage, and sag voltage, the behavior of the power system becomes complex. Single objective function problems are less complex than multi-objective function problems. In this paper, the FPA algorithm has been used for solving the problem efficiently. The proposed UPQC control configuration and the control strategy discussed in the previous section provide the indication of the active component by the d-axis, while the q-axis indicates the reactive component of the load current. The high pass filter was used for filtering both the components. DC-link capacitor voltage was produced by combining both the loss component current of UPQC and the oscillating active current [29].

The shunt was not taking part in the reactive component when the oscillating Q axis current alone was utilized for the generation of the compensation current. Conversely, the phase-locked loop was used for the derivation of the phase angle of the d-axis. The UPQC provided the injected voltage vector when voltage swell or sag occurred in the source.

The reference component of the q-axis was set to '0' whereas the reference component of the d-axis was set to the rated voltage. The transformation block was used for converting the stationary frame to αβ frame while the output was connected to the phase-locked loop. The αβ frame was converted into another transformation block into the dg (rotating) frame, which determined the changes in the axis and phase of the load voltage.

V. RESULT AND DISCUSSION

Simulations were carried out to ensure the performance of the proposed UPQC with FPA under different fault conditions. In this study, two different scenarios, namely, 1) swell and sag voltage and 2) the harmonic distortion and the sag voltage have been considered. The optimized PI controller with UPQC was implemented in MATLAB/SIMULINK and performed in Intel Core i5 with 32 GB RAM computer.

Table- I: Different values used for different faults

Scenarios	Fault points	Fault Type	Fault duration	Fault resistance (Ω)	Fault resistance (Ω)
1	P, Q, R P, Q, R	Swell voltage Sag voltage	0.12-0.22 0.42-0.53	3.3 3.3	0.11 0.11
2	P, Q, R P, Q, R	Sag voltage Non-linear load	0.1-0.2 0.3-0.4	3.3 3.3	0.11 0.11

A. Simulation Setup

Two electrical fault conditions have been considered to enable a study of the performance of the proposed method are listed in Table 1. In the first scenario, the swell and sag voltage occurred between (0.12-0.22 s) and (0.42-0.53 s) respectively. The sag voltage and harmonic distortion that occurred between (0.1-0.2 s) and (0.3-0.4 s) were considered for the second scenario. Various parameters indicated in Table 1, simulated and examined in this study reveal the proposed optimized method rather than that of any other method. Different evolutionary algorithms such as PSO, DE, and ACOA have been used for comparison. Various parameters used in the simulation for the above algorithms are listed in Table 2. The maximum number of iterations is set to 100 for all the algorithms. A dedicated study of the performance of UPQC including PEMFC/SC was made using a classical PI and then applied to the optimization algorithm under different fault conditions. Three PI controllers were used for the q-axis, d-axis, and V_{dc} respectively.

Table- II: Parameters used for different algorithms

PSO	DEA	ACOA	FPA
C_1=1.4 C_{1min}=1 C_2=1.8 C_{2min}=1 W_{max}=1 W_{min}=0.3	F=0.5 CR=0.5 PS=50	β= 10 ρ=0.6 q_o=0.4	P=0.8 β= 1.5

Table- III: Simulated values for scanario-1

Controller	Average voltage sag	Average voltage swell	Power factor	THD (%)
Before compensation	0.4572	1.4924	0.879	2.345
Compensation with classical PI	0.0301	1.0321	0.879	1.092

B. Performance of UPQC including PEMFC/SC

Simulation was performed. The results of not using compensation and compensation with the classical PI controller for the first scenario are presented in Table 3. These show provision of an improvement in voltage sag and THD after the use of classical PI. The power quality index indicated the compensation with classical PI increasing the quality of the power. The simulation result of scenario-2 for not using compensation and compensation with the classical PI controller is shown in Table 4. Table 4 shows that after compensation with classical PI provides an improvement in sag voltage, THD, and an increase in power quality.

The membership function was tuned using the FPA optimization algorithm and the performance was studied. Implementation of PI controller for UPQC with multi-objective function FPA under voltage swell and sag is shown in Fig. 7. The three-phase source voltage was set with 50% of swell and 50% sag occurred in the duration 0.12 s to 0.22 s and 0.42 s to 0.53 s respectively. The source voltage was distorted due to swell and sag in the particular time duration. This is shown in Fig. 7(a). The UPQC acted as a dynamic voltage restorer and injected voltage, V_{UPQC} of 0.5 p.u in the swell duration and 0.5 p.u in the sag duration as shown in Fig. 7 (b). The load voltage and the DC voltage across the hybrid source are shown in Fig. 7 (c) and (d) respectively.

Table- IV: Simulated values for scanario-2

	Average voltage sag	Average voltage swell	Power factor	THD (%)
Before compensation	0.9834	-	0.758	18.517
Compensation with classical PI	0.0438	-	0.826	5.928

The sag voltage was set to 60% and non-linear load was applied for evaluating a study of the performance of the proposed multi-objective FPA method. The three-phase source voltage was set with a 60% sag and non-linear load occurred in the duration 0.12 s to 0.22 s and 0.42 s to 0.53 s respectively.

The optimized PI controller used for UPQC with multi-objective function under voltage sag and non-linear load is shown in Fig. 8. The source voltage was distorted in the duration 0.1 s to 0.2 s and 0.3 s to 0.4 s due to sag and non-linear load. This is shown in Fig. 8(a). The UPQC injected a voltage of 0.6 p.u and the inverter compensated the current in the duration from 0.3 s to 0.4 s is shown in Fig. 8(b).

The load voltage and the DC voltage across the hybrid source are shown in Fig. 8(c) and (d) respectively. The DC-DC boost converter was used for increasing the DC voltage generated by the hybrid source.

C. Performance comparison

The multi-objective optimal controller using the FPA method was implemented in UPQC and analysis with different loads was made for the analysis of the performance of the proposed method.

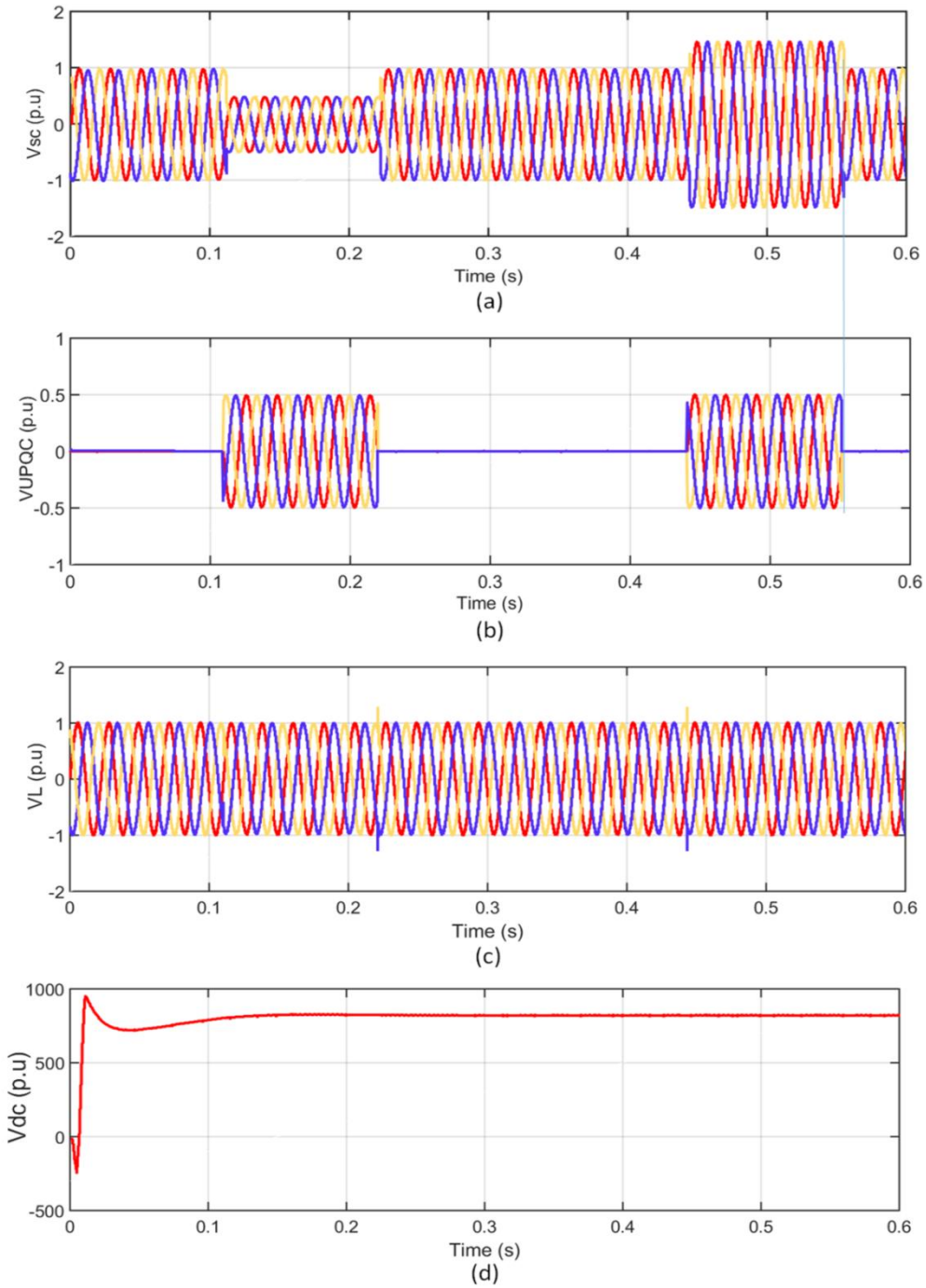

Fig. 7. Performance of multi-objective FPA PI controller based UPQC under 50% sag and swell voltage (a) distorted source voltage due to swell and sag (b) injected voltage by UPQC during swell and sag (c) Load voltage (d) DC voltage of the hybrid source.

Two cases have been considered: 1) inductive load and 2) resistive load. The harmonic spectrum using PSO, DE, ACOA, and the proposed method are shown in Fig. 9. Fig. 9 shows the proposed multi-objective optimized controller making successfully compensation for the THD under 0.73%. The other optimization technique, DE had THD of 1.03% while ACOA had the THD of 1.48%. Consequently, the multi-objective optimal controller based UPQC provided a smaller THD compared to other optimization algorithms.

A comparison of the performance with power quality indices of the proposed multi-objective optimization algorithm was made with other optimization algorithms. This resistive load condition. The IEEE-519 standard range was considered during the simulation. After compensation, the value of THD was 5% less and the proposed algorithm provided the best compensation followed by the PSO that provided

is presented in Table 4. Table 4 shows considerable reduction in the voltage sag and the THD in the proposed multi-objective optimization algorithm. The result shows the effective handling of the compensation problem under different fault conditions by the proposed method.

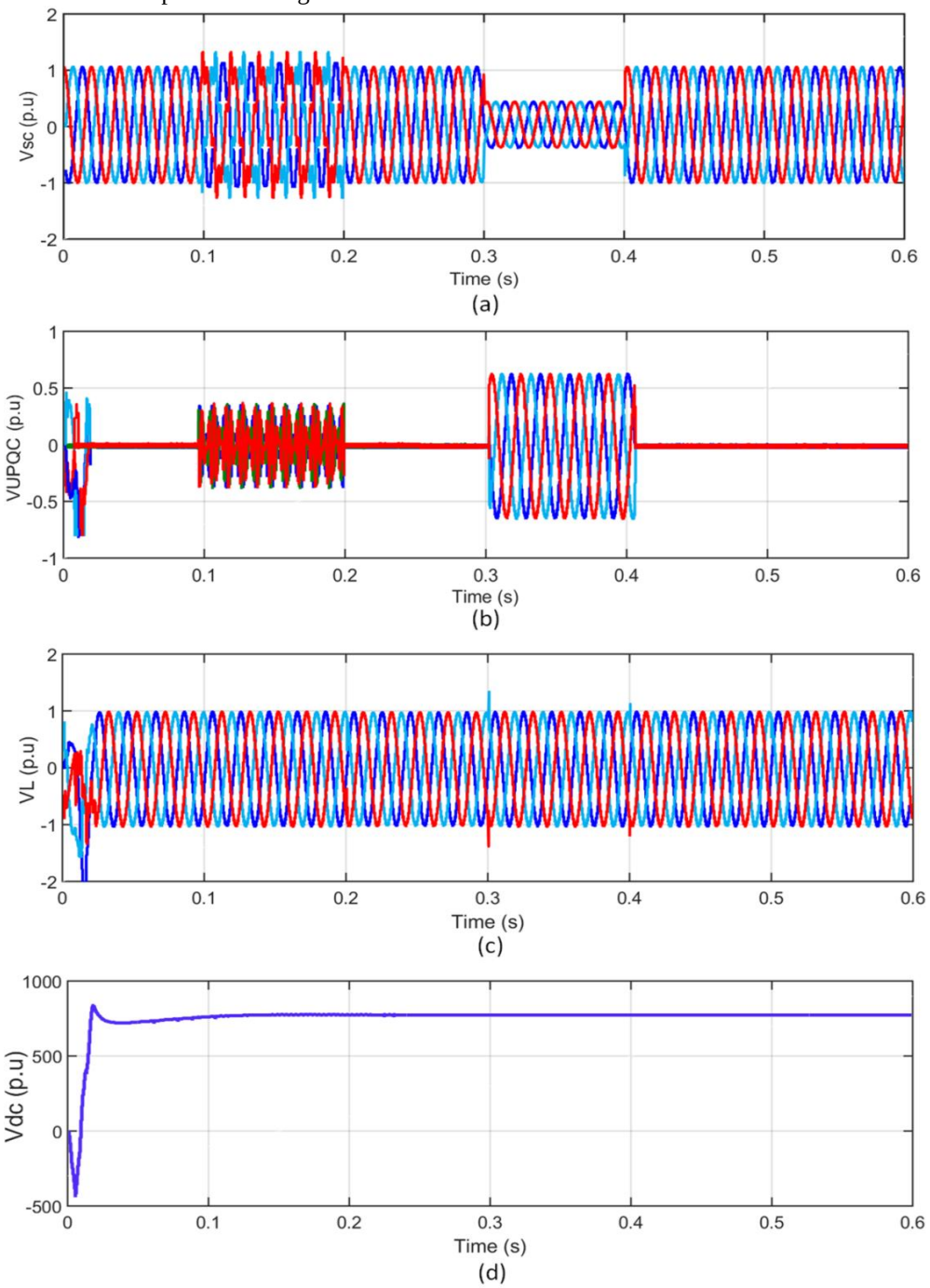

Fig. 8. Performance of multi-objective FPA PI controller based UPQC under 60% voltage sag and non-linear loads (a) distorted source voltage due to swell and sag (b) injected voltage by UPQC during swell and sag (c) Load voltage (d) DC voltage of the hybrid source.

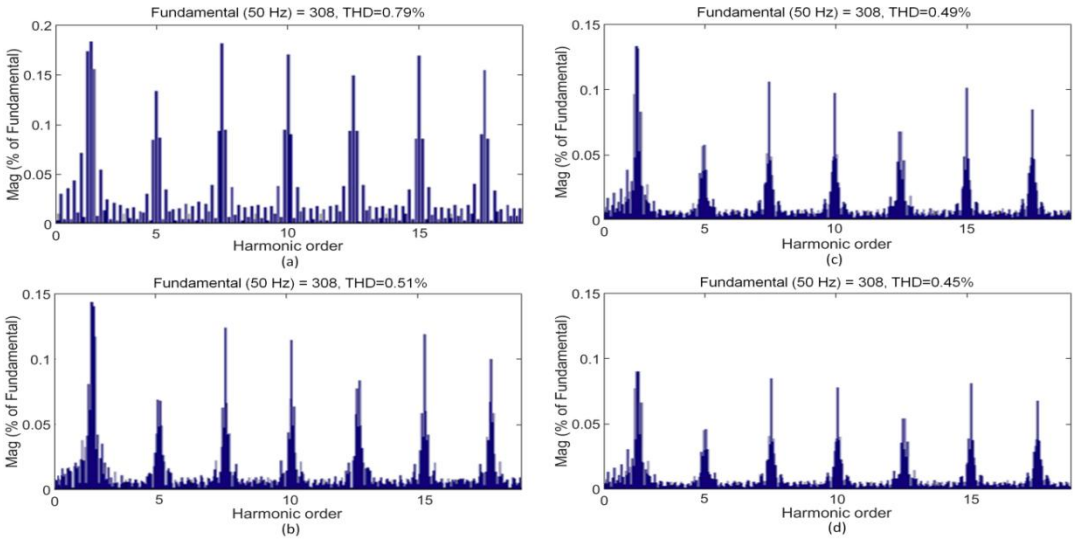

Fig. 9. Harmonic spectrum for different optimization algorithms under resistive loadcondition (a) PSO (b) DE (C) ACOA (d) proposed algorithm.

Table 4. Comparison of power quality indices for case-1.

Controllers	**Average swell voltage**	**Average sag voltage**	**Power factor**	**THD (%)**
Classical PI	1.0427	0.0319	0.861	1.084
Multi-objective PSO	1.0427	0.0208	0.861	0.763
Multi-objective DE	1.0427	0.0183	0.861	0.495
Multi-objective ACOA	1,0427	0.0214	0.861	0.473
Improvement (%)				
Improvement PI-PSO versus PI (%)	-	29.69	-	31.937
Improvement PI-DE versus PI (%)	-	38.37	-	40.372
Improvement PI-ACOA versus PI (%)	-	32.72	-	42.836
Improvement PI-FPA versus PI (%)	-	47.732	-	52.187

Table 5. Comparison of power quality indices for case-2.

Controllers	Average swell voltage	Average sag voltage	Power factor	THD (%)
Classical PI	-	0.0572	0.892	5.836
Multi-objective PSO	-	0.0381	0.924	4.621
Multi-objective DE	-	0.0293	0.918	2.382
Multi-objective ACOA	-	0.0312	0.908	1.683
Improvement (%)				
Improvement PI-PSO versus PI (%)	-	16.37	3.31	3.37
Improvement PI-DE versus PI (%)	-	32.19	3.58	3.72
Improvement PI-ACOA versus PI (%)	-	25.23	4.36	4.24
Improvement PI-FPA versus PI (%)	-	42.82	4.48	4.82

Table 5 shows a comparison of performance with power quality indices of the proposed multi-objective optimization algorithm with other optimization algorithms. Table 5 shows the proposed multi-objective optimization method providing a noticeable improvement in the power quality indices compared to other optimization techniques.

VI. CONCLUSION

In this paper, multi-objective optimization UPQC including the hybrid power source (PEMFC/SC) that acts as a compensating device for the electrical distribution system has been presented. Two different scenarios, namely, swell and sag voltage and the harmonic distortion and the sag voltage have been considered in the study of the performance of the proposed method. Simulation was carried out and the result was compared with three of the different algorithms. The simulation result indicated the multi-objective FPA method based UPQC injecting the desired voltage during the electrical perturbation situation. During the first scenario, the proposed method managed the voltage of both the swell and sag by 50% and, in the second scenario, the sag voltage by 60%. Finally, the comparison result shows improvement in the power quality indices such as swell and sag voltage, THD, and power factor through use of the proposed method.

REFERENCES

1. AK.Panda, N. Patnaik, “Management of reactive power sharing & power quality improvement with SRF-PAC based UPQC under unbalance source voltage condition,” *Int. Journal of Electr. Poer Energy Syst.* Vol. 84, 2017, pp. 182-194.
2. V. Khadkikar, “Enhancing electric power quality using UPQC: a comprehensive review,” *IEEE Trans. Power Etectron.*, vol. 27(5), 2012, pp. 2284-2297.
3. JA Muñoz, JR Espinoza, CR Baier, LA Morán, EE Espinosa, PE Melín, et al. “Design of a discrete-time linear control strategy for a multi cell UPQC,” *IEEE Trans Ind Electron*, vol. 59, 2012, pp. 3797–807.

4. Trinh Q-N, Lee H-H, "Improvement of unified power quality conditioner performance with enhanced resonant control strategy," *IET Gener Transm Distrib*, vol. 8, 2014, pp. 2114–23.
5. Dos Santos RJM, Da Cunha JC, Mezaroba M, "A Simplified Control Technique for a Dual Unified Power Quality Conditione," *IEEE Trans Ind Electron*, vol. 61, 2014, pp. 5851–60.
6. Modesto RA, Da Silva SAO, Jr AA deO, Bacon VD, "A versatile unified power quality conditioner applied to three-phase four-wired distribution systems using a dual control strategy," *IEEE Trans Power* Electron, vol. 31, 2016, pp. 5503–14.
7. Campanhol LBG, Da Silva SAO, Jr AA de O, Bacon VD, "Single-stage three-phase grid tied PV system with universal filtering capability applied to DG systems and AC microgrids," *IEEE Trans Power Electron*, vol. 32, 2017, pp. 9131–42.
8. AxenteI, Ganesh JN, Basu M, Conlon MF, Gaughan K, "A 12-kVA DSP-controlled laboratory prototype UPQC capable of mitigating unbalance in source voltage and load current," *IEEE Trans Power Electron*, vol. 25: 2010, pp. 1471–9.
9. Kwan KH, Chu YC, So PL, "Model-based H control of a unified power quality conditioner," *IEEE Trans Ind Electron*, vol. 56, 2009, pp. 2493–504.
10. De Oliveira FM, Da Silva SAO, Durand FR, Sampaio LP, Bacon VD, Campanhol LBG, "Grid-tied photovoltaic system based on PSO MPPT technique with active power line conditioning," IET Power Electron, vol. 9, 2016, pp. 1180–91.
11. Maccari LA, Santini CLDA, Oliveira RCDLF de, Montagner VF, "Robust discrete linear quadratic control applied to grid-connected converters with LCL filters," *2013 Brazilian Power Electron Conf. COBEP 2013-Proc*., 2013, p.374–9.
12. Chellaswamy C, Muthammal R, Geetha T S, "A New Methodology for Optimal Rail Track Condition Measurement Using Acceleration Signals", Measurement Science and Technology, vol. 29(7), 2018, pp. 1-16..
13. Evran F, "Plug-in repetitive control of single-phase grid-connected inverter for AC module applications," *IET Power Electron*, vol. 10, 2017, pp. 47–58.
14. Zhang G, Huang C, Zhang X, Zhang W, "Practical constrained dynamic positioning control for uncertain ship through the minimal learning parameter technique," *IET Control Theory Appl*, vol.12, 2018, pp. 2526–33.
15. Zhang G, Tian B, Zhang W, Zhang X, "Optimized robust control for industrial unstable process via the mirror-mapping method," *ISA Trans*, vol. 86, 2019, pp. 9–17.
16. Nowak P, Stebel K, Klopot T, Czeczot J, Fratczak M, Laszczyk P, "Flexible function block for industrial applications of active disturbance rejection controller," *Arch Control Sci*, vol. 28, 2018, pp. 379–400.
17. Jinghang Lu, Savaghebi M, GuerreroJ M, Vasquez JC. ChuanXie, "Linear active disturbance rejection control for LCL type grid-connected converter. *IECON 2016–42nd AnnuConf IEEE Ind Electron Soc. 2016*, pp. 3458–63.
18. Kanjiya P, Singh B, Chandra A, AI-Haddad K, SRF Theory Revisited to control self-supported dynamic voltage restorer (DVR) for unbalanced and nonlinear loads," *IEEE Trans Ind. Appl*, vol. 49(5), 2013, pp. 2330-40.
19. Satya Dinesh Madasu, M.L.S. Sai Kumar, Arun Kumar Singh, "A flower pollination algorithm based automatic generation control of interconnected power system," *Ain Shams Engineering Journal*, vol. 9, 2018, pp. 1215-1224.
20. Eyad S. Oda, Abdelazeem A. Abdelsalam, Mohamed N. Abdel-Wahab, Magdi M.El-Saadawi, "Distributed generations planning using flower pollination algorithm for enhancing distribution system voltage stability," *Ain Shams Engineering Journa*l, vol. 8(4), 2017, pp. 593-603.
21. Kaliraja T, Martin Leo Manickam, Chellaswamy C, **"**An experimental study on photovoltaic module with optimum power point tracking method," *International Transactions on Electrical Energy Systems*, e12175, pp. 1-26, 2019.
22. Brahim Berbaoui, "Optimal capacity of energy storage for dynamic voltage restorer under electrical faults scenarios using SOS optimization algorithm: case of south Algerian's electrical autonomous grid application," *J Energy Storage*, vol. 14, 2017, pp. 134-46.
23. A. Obara, "Equipment plan of compound interconnection micro-grid composed from diesel power plants and solid polymer membrane-type fuel cell," *Int J Hydrogen Energy*, vol. 33(1), 2008, pp. 179-88.
24. N. Patnaik, AK. Panda, "Performance analysis of a 3-phase 4 wire UPQC system based on PAC based SRF controller with real time digital simulation," *Int J Electr Power Energy Syst*. Vol. 74, 2016, pp. 212-21.
25. A. Jeraldine Viji, T. Aruldoss Albert Victoire, "Enhanced PLL based SRF control method for UPQC with fault protection under unbalanced load conditions," *Int J Electr Power Energy Syst*., vol. 58, 2014, pp. 319-28.
26. I. Axente, M. Basu, MF Conlon, "Dc link voltage control of UPQC for better dynamic performance," *Electr Power Syst Res*, vol. 81(9), 2011, pp. 1815-24.
27. Patjoshi RK, Mahapatra K, "High-performance unified power quality conditioner using command generator tracker-based direct adaptive control strategy," *IET Power Electron*, vol. 9(6), 2016, pp. 1267-78.
28. RK Patjoshi, K. Mahapatra, "High-performance unifiedpowerquality conditioner using non-linear sliding mode and new switching dynamics control strategy," *IET Power Electron*, vol. 10(8), 2017, pp. 863-74.
29. Rauf AM, Sant AV, Khadkikar V, Zeineldin HH, "A novel ten-switch topology for unified power quality conditioner," *IEEE Trans Power Electron*, vol. 31(10), 2016, pp. 6937-46.
30. Li Tianyu, Liu Huiying, Zhao Dingxuan, Wanga Lili, "Design and analysis of a fuel cell supercapacitor hybrid construction vehicle," *Int J Hydrogen Energy*, vol. 41(28), 2016, pp. 12307-19.
31. CK. Sundarabalan, K. Selvi, "Real coded GA optimized fuzzy logic controlled PEMFC based Dynamic Voltage Restorer for reparation of voltage disturbances in distribution system," *Int J Hydrogen Energy*, 2016.
32. N. Mebarki, T. Rekioua, Z. Mokrani, D. Rekioua, S. Bachab, "PEM fuel cell/battery storage system supplying electric vehicle," I*nt J Hydrogen Energy*, vol. 41(45), 2016, pp. 20993-1005.
33. Y. Zhan, Y. Guo, J. Zhu, L. Li, "Power and energy management of grid/PEMFC/battery/supercapacitor hybrid power sources for UPS applications," *Int J Electr Power Energy Syst*, vol. 67, 2015, pp. 598-612.
34. Martín Alfredo Ursúa Pablo Sanchis Idoia San, "Integration of fuel cells and supercapacitors in electrical microgrids: analysis, modelling and experimental validation, "*Int J Hydrogen Energy*, vol. 38(27), 2013, pp. 11655-71.
35. Chellaswamy C and Ramesh R, "An optimal parameter extraction and crack identification method for solar photovoltaic modules", *ARPN Journal of Engineering and Applied Sciences*, vol. 11(24), 2016, pp. 14468-14481.
36. H. Falaghi, MR. Haghifam, C. Singh, "Ant colony optimization-based method for placement of sectionalizing switches in distribution networks using a fuzzy multi objective approach," *IEEE Trans Power Deliv*, vol. 24(1), 2009, pp. 268e76.

AUTHORS PROFILE

K. Hussain completed his B.Tech (EEE) from JNTU College of Engineering, Hyderabad in 2001 and M.Tech (Control Systems) from N.I.T. Kurukshetra, Haryana in 2003 and Ph.D. in Power Systems from SR University, Rajasthan in 2018. He is presently working as Associate Professor and Head of the department of Electrical Engineering, Sharad Institute of Technology College of Engineering, Yadrav (Ichalkaranji), Kolhapur, Maharashtra. He has published 8 papers in International Journals, 2 international conferences and 2 papers in National Conferences. His research interests are Power Systems, Power Electronics and Control Systems. He is a Senior Member of IEDRC and member of IAENG.

Puli Sridhar was born in Andhra Pradesh, India, in 1979. He Received B. Tech Degree in Electrical and Electronics Engineering from JNTUCEH, Hyderabad, Telangana, India in 2001. M. Tech Degree in Electrical Power Systems from JNTUCEH, Hyderabad, Telangana, India in 2006 and Ph.D. in Power Systems from Sunrise University, Alwar, Rajasthan, India in 2018. He is currently working as Professor in Department of Electrical and Electronics Engineering, TRR College of Engineering, Patancheru, Telangana, India. He is Life Member of the Indian Society for Technical Education (ISTE). Email: sridhar122879@gmail.com